BeppoSAX Observations of Unprecedented Synchrotron Activity in the BL Lac Object Mkn 501

Elena Pian[1,2], Giuseppe Vacanti[3], Gianpiero Tagliaferri[4], Gabriele Ghisellini[4],

Laura Maraschi[5], Aldo Treves[6], C. Megan Urry[1], Fabrizio Fiore[7], Paolo Giommi[7],

Eliana Palazzi[2], Lucio Chiappetti[8], Rita M. Sambruna[9]

electronic addresses: pian@stsci.edu; gvacanti@astro.estec.esa.nl; gtagliaf@astmim.mi.astro.it; gabriele@merate.mi.astro.it; maraschi@brera.mi.astro.it; treves@astmiu.mi.astro.it; cmu@stsci.edu; fiore@sax.sdc.asi.it; giommi@sax.sdc.asi.it; eliana@tesre.bo.cnr.it; lucio@ifctr.mi.cnr.it; rms@latte.astro.psu.edu

ABSTRACT

The BL Lac object Mkn 501, one of the only three extragalactic sources (with Mkn 421 and 1ES 2344+514) so far detected at TeV energies, was observed with the BeppoSAX satellite on 7, 11, and 16 April 1997 during a phase of high activity at TeV energies, as monitored with the Whipple, HEGRA and CAT Cherenkov telescopes. Over the whole 0.1-200 keV range the spectrum was exceptionally hard ($\alpha \leq 1$, with $F_\nu \propto \nu^{-\alpha}$) indicating that the X-ray power output peaked at (or above) ~100 keV. This represents a shift of at least two orders of magnitude with respect to previous observations of Mkn 501, a behavior never seen before in this or any other blazar. The overall X-ray spectrum hardens with increasing intensity and, at each epoch, it is softer at

[1]Space Telescope Science Institute, 3700 San Martin Drive, Baltimore, MD 21218

[2]ITESRE-CNR, Via Gobetti 101, I-40129 Bologna, Italy

[3]ESA ESTEC, Space Science Department, Astrophysics Division, Postbus 299, NL-2200 AG Noordwijk, The Netherlands

[4]Osservatorio Astronomico di Brera, Via Bianchi 46, I-22055 Merate (Lecco), Italy

[5]Osservatorio Astronomico di Brera, Via Brera 28, I-20121 Milan, Italy

[6]Department of Physics, University of Milan at Como, Via Lucini 3, I-22100 Como, Italy

[7]SAX SDC, Via Corcolle 19, I-00131, Rome, Italy

[8]IFCTR-CNR, Via Bassini 15, I-20133 Milan, Italy

[9]NASA/Goddard Space Flight Center, Greenbelt, MD 20771

larger energies. The correlated variability from soft X-rays to the TeV band points to models in which the same population of relativistic electrons produces the X-ray continuum via synchrotron radiation and the TeV emission by inverse Compton scattering of the synchrotron photons or other seed photons. For the first time in any blazar the synchrotron power is observed to peak at hard X-ray energies. The large shift of the synchrotron peak frequency with respect to previous observations of Mkn 501 implies that intrinsic changes in the relativistic electron spectrum caused the increase in emitted power. Due to the very high electron energies, the inverse Compton process is limited by the Klein-Nishina regime. This implies a quasi-linear (as opposed to quadratic) relation of the variability amplitude in the TeV and hard X-ray ranges (for the SSC model) and an increase of the inverse Compton peak frequency smaller than that of the synchrotron peak frequency.

Subject headings: BL Lacertae objects: individual (Mkn 501) — galaxies: active — galaxies: nuclei — radiation mechanisms: non-thermal — X-rays: galaxies

1. Introduction

Mkn 501 is one of the closest (z=0.034) BL Lacertae objects, and one of the brightest at all wavelengths. It was the second source, after Mkn 421, to be detected at TeV energies by the Whipple and HEGRA observatories (Quinn et al. 1996; Bradbury et al. 1997). Historically, its spectral energy distribution (νF_ν) resembles that of BL Lac objects selected at X-ray energies, having a peak in the EUV-soft X-ray energy band. Such objects were defined as High-frequency-peaked BL Lacs, or HBL, by Padovani & Giommi (1995). In fact, the 2–10 keV spectra observed so far were relatively steep, with energy spectral indices α larger than unity ($F_\nu \propto \nu^{-\alpha}$), meaning the power output peaks below this band. From the EXOSAT data base the hardest X-ray spectrum of Mkn 501, measured in one of its brightest states, had a spectral index of 1.2 ± 0.1 (Sambruna et al. 1994). *Einstein* measured in two occasions spectral indices consistent with values smaller than 1 within the large errors (Urry, Mushotzky, & Holt 1986).

Mkn 501 was observed with BeppoSAX over a period of ∼10 hours on each 7, 11, and 16 April 1997, during a multiwavelength campaign involving ground-based TeV Cherenkov telescopes (Whipple, HEGRA and CAT), plus other satellites, CGRO (EGRET and OSSE), RXTE, ISO, and optical telescopes. First results on the TeV observations are presented in Catanese et al. (1997), Aharonian et al. (1997a), Barrau et al. (1997). Infrared, optical,

and radio data from the multiwavelength campaign, as well as a complete analysis of the BeppoSAX data, including a detailed study of the intraday X-ray variability, will be presented in forthcoming papers. Here we concentrate on the average spectra obtained during the three BeppoSAX pointings. In the X-ray band, unprecedented spectral behavior is observed, offering new constraints on blazar emission mechanisms.

2. Observations, analysis, and results

A complete description of the BeppoSAX mission is given by Boella et al. (1997). Mkn 501 was observed with the LECS (0.1–10 keV), the MECS (1.5–11 keV), and the PDS (13-300 keV). Event files of the three BeppoSAX pointings for the LECS and MECS experiments were linearized and cleaned with SAXDAS at the BeppoSAX Science Data Center (SDC; Giommi & Fiore 1997). Light curves and spectra were accumulated for each pointing with the SAXSELECT tool, using 8.5 and 4 arcmin extraction radii for the LECS and the MECS, respectively, that provide more than 90% of the fluxes. The background intensity was evaluated from files accumulated from blank fields available at the SDC. For each of the four PDS units, source+background and background spectra were accumulated using the XAS software package, after selecting the source visibility windows. The target was significantly detected up to the highest energy channels. Each net spectrum was binned in energy intervals to reach a signal-to-noise ratio larger than 20, up to 150 keV. The grouped spectra from the four units were then coadded.

Spectral analysis was performed with the XSPEC 9.01 package, using for each instrument the response matrices released by the SDC. LECS data have been considered only in the range 0.1–4 keV, due to still unsolved calibration problems at higher energies, and MECS data in the range 1.8–10.5 keV. For each observation, the LECS and MECS spectra have been jointly fit after allowing for a constant, systematic rescaling factor of the LECS data, to account for uncertainties in the intercalibration of the instruments (Parmar 1997), which had a best fit value of 0.64. We considered both simple and broken power-law models; the latter is appropriate for HBL, which often show downward curved spectra. With the former model, the fitted $N_{\rm H}$ is 30-40% higher than the Galactic value (1.73×10^{20} cm^{-2}; Elvis, Lockman, & Wilkes 1989), while the broken power-law model yields a value equal to the Galactic one for the first two observations and a somewhat lower value ($\sim$ 20%) for the third one. We then fixed $N_{\rm H}$ at the Galactic value and determined the best-fit parameters for both the single and broken power-law models (see Table 1): the latter is clearly in all cases a better representation of the data (the χ^2 improvement is highly significant as estimated from the F-test). The spectral steepening between the LECS

and MECS bands is of $\Delta\alpha \simeq 0.2 - 0.3$ at all epochs. Single power-laws represent well the PDS spectra in the 13–200 keV range (see fit parameters in Table 1) at each epoch. For 7 and 11 April the PDS slopes are consistent with the energy indices derived from the broken power-law LECS+MECS best-fits (α_2 in Table 1), while for 16 April the spectrum in the 13–200 keV band is significantly steeper than in the MECS band. After rescaling the PDS data by a factor 0.75 to take into account a calibration mismatch with respect to the MECS response, we fit the 16 April spectrum over the whole range (LECS+MECS+PDS) with a broken power-law model. The PDS data show a systematic deviation from the model (Fig. 1a), indicating a further steepening at higher energies. Figure 1b shows a joint fit only to the MECS+PDS data with a broken power-law with break energy of ~ 20 keV: the spectral indices on the lower and higher energy side of the break (see figure caption) are similar to α_2 and α_{PDS} (Table 1), respectively.

In order to characterize the spectral variability in the full range independently of calibration uncertainties or model assumptions, we computed the ratio of the count rates observed on 16 April to those observed on 7 April vs. energy, as shown in Figure 2. It is clear that the variability is systematically larger at higher energies implying an overall hardening of the spectrum with increasing intensity, by about $\Delta\alpha \simeq 0.2$ (see Table 1). On 7 and 11 April the spectral index in the PDS band is consistent with $\alpha \simeq 1$, while on 16 April it is less than unity, indicating that the peak of the power output falls in the PDS band at the first two epochs but is at the extreme end of the PDS band or beyond in the highest intensity state.

3. Spectral energy distribution

In Figure 3 the unfolded and unabsorbed X-ray spectra from the BeppoSAX observations of 7 and 16 April 7 are compared with previously observed X-ray spectra in three brightness states and with data from the radio to the TeV range (see figure caption for references). The present X-ray observations imply a dramatic hardening of the spectral energy distribution in the medium X-ray band and an increase of the (apparent) bolometric luminosity of a factor ≥ 20 with respect to previous epochs. The really striking feature is that the peak of the power output (i.e., where $\alpha = 1$) is found to *have shifted* in energy by a factor ≥ 100. Moreover for the first time in any blazar the peak is observed to *occur in the hard X-ray range*, definitely above $\sim 50 - 100$ keV (cf. Ulrich, Maraschi, & Urry 1997). Since in the optical the source was nearly normal (Buckley & McEnery 1997) the change of the spectral energy distribution seems to be confined to energies greater than $\sim$0.1 keV, as also indicated by the apparent pivot of the three BeppoSAX spectra. The overall continuity

of the X-ray spectra reported here with previous UV and soft X-ray measurements suggests that the X-ray emission constitutes the high energy end of the synchrotron component and thus that its peak frequency increased by more than two orders of magnitude and its power by more than one order of magnitude with respect to previous observations of Mkn 501.

The TeV emission also brightened by more than a factor of 5 in the first two weeks of April, with the most intense TeV flare peaking on 16 April (Catanese et al. 1997), the date of the last BeppoSAX observation. However, unlike the X-ray spectrum, the TeV spectrum was steeper than $\alpha = 1$ and did not show noticeable temporal variation; from the HEGRA measurements during the period March-April and during the more active period 7-13 April, the spectral index above 1 TeV remained unchanged, within the large errors ($\Delta\alpha \sim 0.3$), with an average value $\alpha \simeq 1.5$ (Aharonian et al. 1997a,b). At the same time, Mkn 501 was not detected by EGRET (Catanese et al. 1997), indicating that the γ-ray flare is modest at a few GeV. This constrains the peak power output of the very high energy component to occur between the GeV and TeV ranges. Note that also during the quiescent state the latter peak was poorly constrained so that it is difficult to make a strong statement about a possible shift. In the quiescent state the TeV flux was a factor $\sim$100 less than during the flare of 16 April.

4. Model implications

The spectral energy distribution of HBL can be well explained by the synchrotron self-Compton model, in which the dominant source of seed photons is the synchrotron emission (Jones, O'Dell, & Stein 1974; Ghisellini, Maraschi, & Dondi 1996; Mastichiadis & Kirk 1997). If the energy distribution of the emitting electrons, $N(\gamma)$, changes at the highest energies, this model explains naturally the correlated flaring at X-ray and TeV energies, with the highest energy electrons producing X-rays via synchrotron and the TeV radiation via inverse Compton scattering. Because of the very high electron energies involved, the scattering cross section for energetic photons is reduced by the Klein-Nishina effect and only photons below the Klein-Nishina threshold ($h\nu \leq mc^2/\gamma$) are effectively upscattered. This means that (i) the inverse Compton flux does not vary more than the synchrotron flux from the same electrons, since the available seed photons are limited (Ghisellini & Maraschi 1996) and (ii) the peak of the inverse Compton power shifts less in frequency than the synchrotron peak.

The shift of $\sim$2 orders of magnitude in the frequency ν_S of the synchrotron peak of Mkn 501 cannot be ascribed to either a variation of Doppler factor, δ, or magnetic field, B, alone; enormous variations would be demanded, since $\nu_S \propto B\delta$, and these changes would

affect other parts of the spectrum quite strongly in a way that is not observed. Therefore, a real change in power and an increase in maximum electron energy, γ_{max}, is implied. Assuming that the power variation is only due to a change in the electron energy, γ_{max} must have increased by roughly a factor of $\sim$10–30. The corresponding shift of the inverse Compton peak is expected to be of the same order of magnitude, being in the Klein-Nishina regime. Since the cooling time of these very high energy electrons is rather short and the synchrotron peak did not move back to the quiescent position during at least 10 days, a mechanism of continuous particle injection is required. This could be impulsive acceleration of electrons at a shock, which might be triggered by fluctuations in the velocity or energy of newly injected plasma. In the γ-ray emitting region, the fresh electrons would therefore scatter, besides the synchrotron photons, also a pre-existing (and more stationary) photon population, produced by an older electron distribution. The hard X-ray and TeV emission should then vary with similar amplitude, while the flux in the infrared-optical band could remain almost stationary.

Three one-zone synchrotron self-Compton models along these lines are shown in Figure 3 for the quiescent state and the 7 and 16 April states. The $N(\gamma)$ distribution has been found self-consistently solving the continuity equation including continuous injection of relativistic particles, radiative losses, electron-positron pair production and taking into account the Klein-Nishina cross section (Ghisellini 1989). The parameters of the fits are given in the figure caption. A variation of the maximum energy of the emitting electrons, together with an increased luminosity and a flattening of the injected particle distribution can describe the observed flaring spectra quite well. We assumed that the seed photons for the inverse Compton scattering are the sum of those produced by the injected electrons plus a stationary component, comparable to the observed infrared-optical flux, which is assumed to be cospatial with the high energy emission. This component can be associated with the "quiescent" spectrum. We recall that these one-zone models cannot account for the radio emission, thought to be produced in much larger regions of the source.

We note that the soft X-ray flux (up to a few keV) did not vary dramatically, and soft X-ray observations alone would have failed to recognize an unusual behavior, except for measuring a spectral inversion, namely a change in slope from values larger than 1 to values smaller than 1. In the EXOSAT data base (Sambruna et al. 1994) at least two sources (out of 16) show spectral indices smaller than 1 in the medium energy X-ray range, but in the brightest and most frequently observed sources (i.e., with more than 10 spectra, which is the case also for Mkn 501) such behavior was never observed. Thus flares as discovered in Mkn 501 may occur in other (similar) blazars though not very frequently and/or some blazars may be more often in ultra-hard states. The signature would be a flat slope in the X-rays, with a flux level consistent with the extrapolation of the infrared-optical synchrotron

spectrum. These sources should be the most variable in hard X-rays and the strongest ones in the TeV band, therefore, their investigation with the existing and rapidly developing X- and γ-ray instrumentation is one of the most promising projects of high energy astronomy.

We thank F. Aharonian for a critical reading of the manuscript and for providing helpful comments and suggestions, and M. Catanese for sending us, on behalf of the Whipple team, his manuscript in advance of submission. J. Buckley, G. Fossati, K. O'Flaherty, M. Schubnell, T. Weekes are acknowledged for their support of this project. CMU and Elena Pian acknowledge support from NASA grants NAG5-2510 and NAG5-2538.

REFERENCES

Aharonian, F., et al. 1997a, A&A, submitted

Aharonian, F., et al. 1997b, in Proc. of the 4th Compton Symposium, Williamsburg, 27-30 April 1997, in press

Barrau, A., et al. 1997, 25th ICRC, Durban (astro-ph/9705249)

Bloom, S. D., & Marscher, A. P. 1991, ApJ, 366, 16

Boella, G., Butler, R. C., Perola, G. C., Piro, L., Scarsi, L., & Bleeker, J. A. M. 1997, A&AS, 122, 299

Bradbury, S. M., et al. 1997, A&A, 320, L5

Breslin, A. C., et al. 1997, IAU Circ. No. 6592

Buckley, J., & McEnery, J. 1997, in preparation

Burbidge, G., & Hewitt, A. 1987, AJ, 93, 1

Catanese, M., et al. 1997, ApJ, 487, L143

Comastri, A., Fossati, G., Ghisellini, G., & Molendi, S. 1997, ApJ, 480, 534

Elvis, M., Lockman, F. J., & Wilkes, B. J. 1989, AJ, 97, 777

Gear, W. K., et al. 1994, MNRAS, 267, 167

Ghisellini, G. 1989, MNRAS, 236, 341

Ghisellini, G., Maraschi, L., & Dondi, L. 1996, A&AS, 120, 503

Ghisellini, G., & Maraschi, L. 1996, in Blazar Continuum Variability, ASP Conf. Ser. Vol. 110, eds H. R. Miller, J. R. Webb, and J. C. Noble, p. 436

Giommi, P., & Fiore, F. 1997, Proc. of 5th International Workshop on Data Analysis in Astronomy, Erice, in press

Impey, C. D., & Neugebauer, G. 1988, AJ, 95, 307

Jones, T. W., ODell, S. L., & Stein, W. A. 1974, ApJ, 188, 353

Lawrence, A., Rowan-Robinson, M., Efstathiou, A., Ward, M. J., Elvis, M., Smith, M. G., Duncan, W. D., & Robson, E. I. 1991, MNRAS, 248, 91

Mastichiadis, A., & Kirk, J. G. 1997, A&A, 320, 19

Padovani, P., & Giommi, P. 1995, ApJ, 444, 567

Parmar, A. N. 1997, private communication

Pian, E., & Treves, A. 1993, ApJ, 416, 130

Quinn, J., et al. 1996, ApJ, 456, L83

Sambruna, R. M., Barr, P., Giommi, P., Maraschi, L., Tagliaferri, G., & Treves, A. 1994, ApJS, 95, 371

Steppe, H., Salter, C. J., Chini, R., Kreysa, E., Brunswig, W., & Lobato Perez, J. 1988, A&AS, 75, 317

Ulrich, M.-H., Maraschi, L., & Urry, C. M. 1997, ARA&A, in press

Urry, C. M., Mushotzky, R. F., & Holt, S. S. 1986, ApJ, 305, 369

Véron-Cetty, M.-P., & Véron, P. 1993, ESO Scientific Report No. 13, 1

Weekes, T. C., et al. 1996, A&AS, 120, 603

Wiren, S., Valtaoja, E., Teräsranta, H., & Kotilainen, J. 1992, AJ, 104, 1009

Worrall, D. M., & Wilkes, B. J. 1990, ApJ, 360, 396

Figure Captions

Fig. 1.— *a)* Broken power-law fit to the LECS+MECS+PDS data of 16 April 1997. The top panel shows the spectra from each instrument (see Table 1 for the parameters); the bottom panel shows the ratio between the spectral flux distribution and the model; *b)* same as in *(a)* for the MECS+PDS data of 16 April: best fit spectral indices at energies lower and higher than the break energy of $19.5^{+4.5}_{-3.5}$ keV are $0.58^{+0.03}_{-0.02}$ and $0.83^{+0.08}_{-0.06}$, respectively ($\chi^2_r = 1.24$ for 113 degrees of freedom).

Fig. 2.— Ratio of the LECS+MECS+PDS spectra of 7 and 16 April. The hardening of the 16 April spectrum is clearly evident.

Fig. 3.— Spectral energy distribution of Mkn 501. BeppoSAX data from 7 and 16 April 1997 are indicated as labeled. Nearly simultaneous Whipple TeV data (from Catanese et al. 1997) are indicated as filled circles, while the open circle (13 April 1997) and the TeV spectral fit (15-20 March 1997) along with its 1-σ confidence range are from the HEGRA experiment (Aharonian et al. 1997a). Non-simultaneous measurements collected from the literature are shown as open squares (radio, Gear et al. 1994; millimeter, Steppe et al. 1988, Wiren et al. 1992, Lawrence et al. 1991, Bloom & Marscher 1991; far-infrared Impey & Neugebauer 1988; optical, Véron-Cetty & Véron 1993, Burbidge & Hewitt 1987; UV, Pian & Treves 1993; TeV, Quinn et al. 1996, Breslin et al. 1997, Bradbury et al. 1997). X-ray spectral fits in the low state are from Sambruna et al. (1994), Worrall & Wilkes (1990), Comastri et al. (1997). Upper limits at 100 MeV are from Weekes et al. (1996), Catanese et al. (1997). The solid lines indicate fits with a one-zone, homogeneous synchrotron self-Compton model. For all models the size of the emitting region is $R = 5 \times 10^{15}$ cm, the beaming factor is $\delta = 15$ and the magnetic field is $B \sim 0.8$ Gauss. For the "quiescent state", the intrinsic luminosity (corrected for beaming) is $L' = 4.6 \times 10^{40}$ erg s^{-1}, and electrons are continuously injected with a power-law distribution ($\propto \gamma^{-2}$) between $\gamma_{min} = 3 \times 10^3$ and $\gamma_{max} = 6 \times 10^5$. For the fit to the 7 April spectrum, $L' = 1.8 \times 10^{41}$ erg s^{-1} and the injected electron distribution ($\propto \gamma^{-1.5}$) extends from γ^4_{min} to $\gamma_{max} = 3 \times 10^6$. For the fit to the 16 April spectrum, $L' = 5.5 \times 10^{41}$ erg s^{-1} and the injected electron distribution ($\propto \gamma^{-1}$) extends from $\gamma_{min} = 4 \times 10^5$ to $\gamma_{max} = 3 \times 10^6$. For the 7 and 16 April models, the seed photons for the Compton scattering are the sum of those produced by the assumed electron distribution plus those corresponding to the quiescent spectrum.

Table 1: Spectral fits[a] to LECS+MECS and PDS data

Obs. Start-End[b]	7.2295-7.6679	11.2458-11.6846	16.1506-16.6082
α^c	0.80 ± 0.01	0.74 ± 0.01	0.52 ± 0.01
χ^2_r ($N_{d.o.f.}$)	3.4 (180)	1.78 (180)	2.77 (180)
α^d_1 ($E < E_{break}$)	0.63 ± 0.04	$0.64^{+0.02}_{-0.04}$	$0.40^{+0.02}_{-0.04}$
α^d_2 ($E > E_{break}$)	0.91 ± 0.02	0.80 ± 0.02	$0.59^{+0.02}_{-0.01}$
E_{break} (keV)	$1.76^{+0.24}_{-0.22}$	1.85 ± 0.33	$2.14^{+0.30}_{-2.14}$
χ^2_r ($N_{d.o.f.}$)	1.29 (178)	1.00 (178)	1.33 (178)
α_{PDS}	0.99 ± 0.13	$0.83^{+0.09}_{-0.08}$	$0.84^{+0.03}_{-0.04}$
χ^2_r ($N_{d.o.f.}$)	0.92 (12)	1.60 (12)	1.09 (12)
$S^e_{0.1-2keV}$	1.75 ± 0.01	1.75 ± 0.01	2.55 ± 0.01
$S^e_{2-10keV}$	2.20 ± 0.01	2.45 ± 0.01	5.35 ± 0.01
$S^e_{13-200keV}$	3.75 ± 0.15	5.15 ± 0.15	15.8 ± 0.2

[a] $F_\nu \propto \nu^{-\alpha}$. Errors are at 90% confidence level for one ($\Delta\chi^2 = 2.71$) or three ($\Delta\chi^2 = 6.1$) parameters of interest.

[b] Day of April 1997.

[c] Energy index from the single power-law fit to combined LECS and MECS data.

[d] Energy index from the broken power-law fit to combined LECS and MECS data.

[e] Unabsorbed intensities, in units of 10^{-10} erg s^{-1} cm^{-2}, derived from the broken power-law model fit.

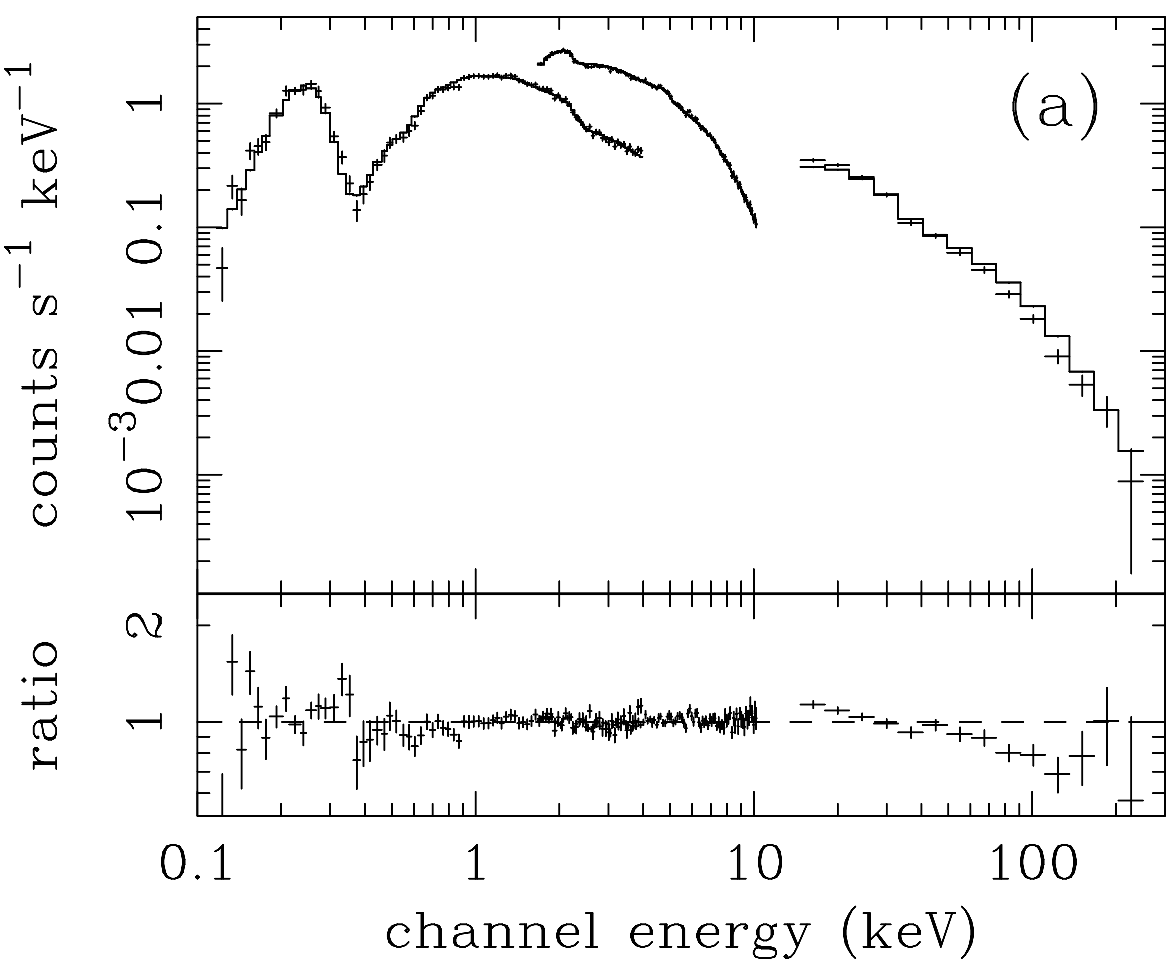

(a)
counts s^{-1} keV^{-1}
1
0.1
0.01
10^{-3}
ratio
2
1
0.1
1
10
100
channel energy (keV)

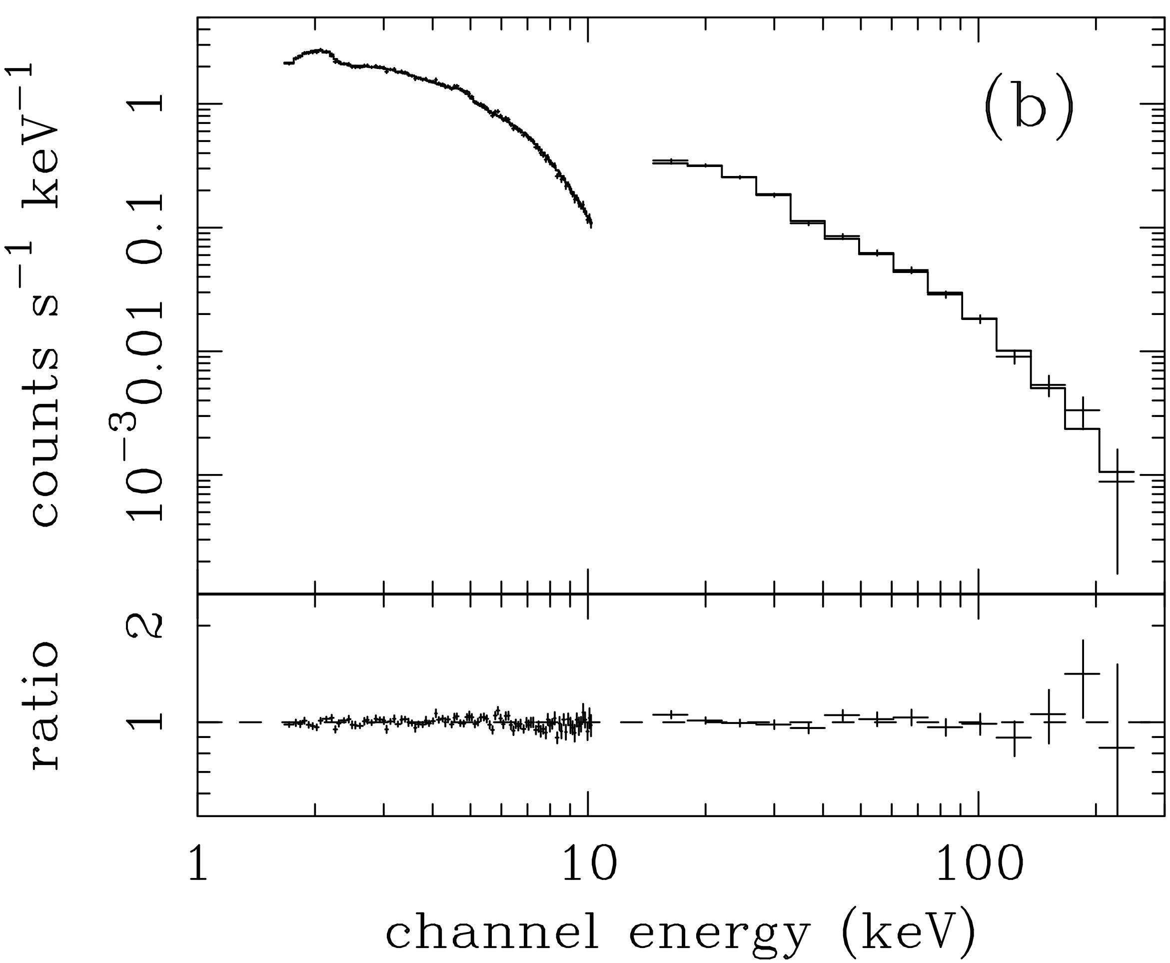
(b)
counts s^{-1} keV^{-1}
1
0.1
0.01
10^{-3}
ratio
2
1
1
10
100
channel energy (keV)

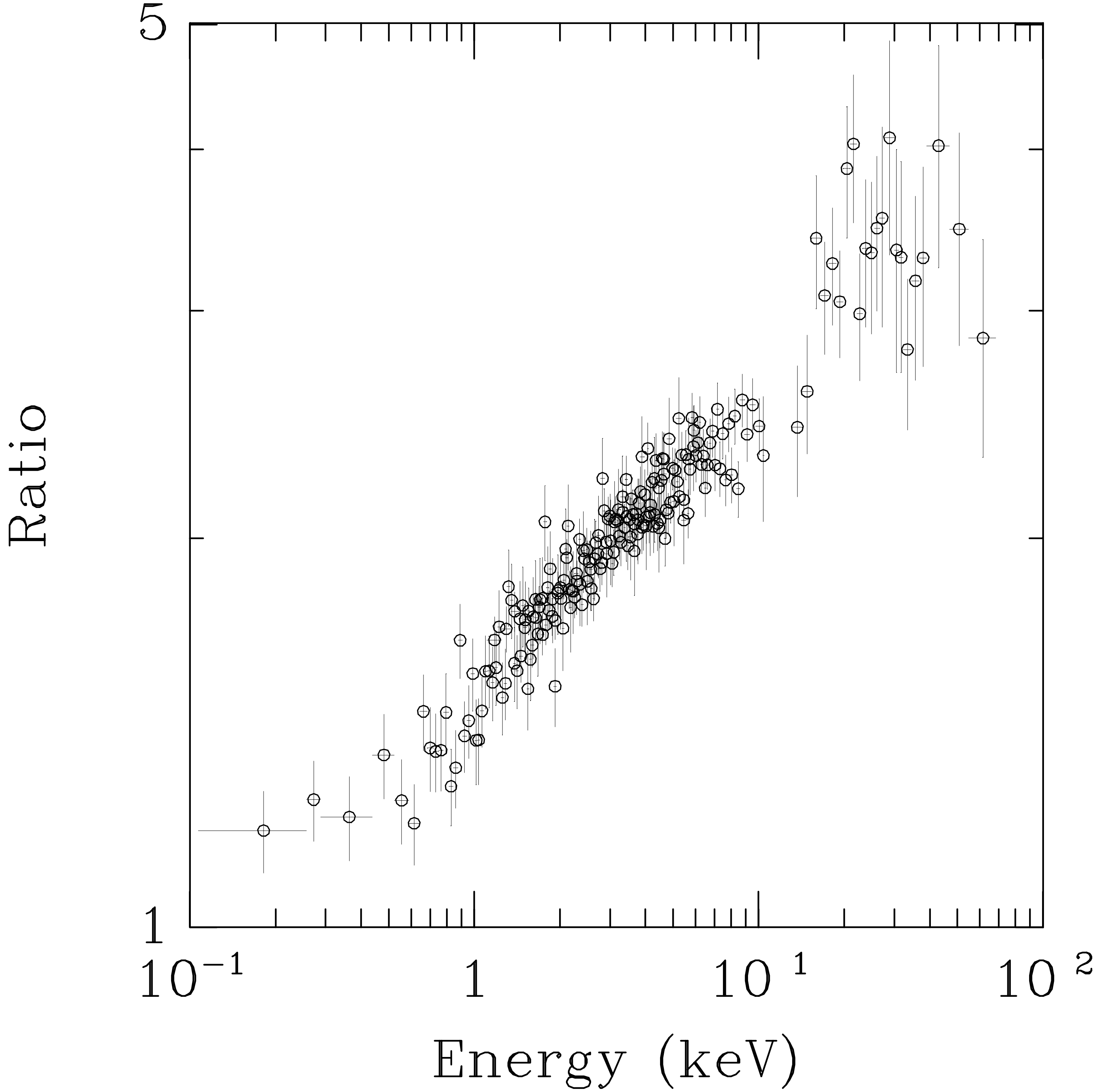

5
1
Ratio
10−1
1
10 1
10 2
Energy (keV)

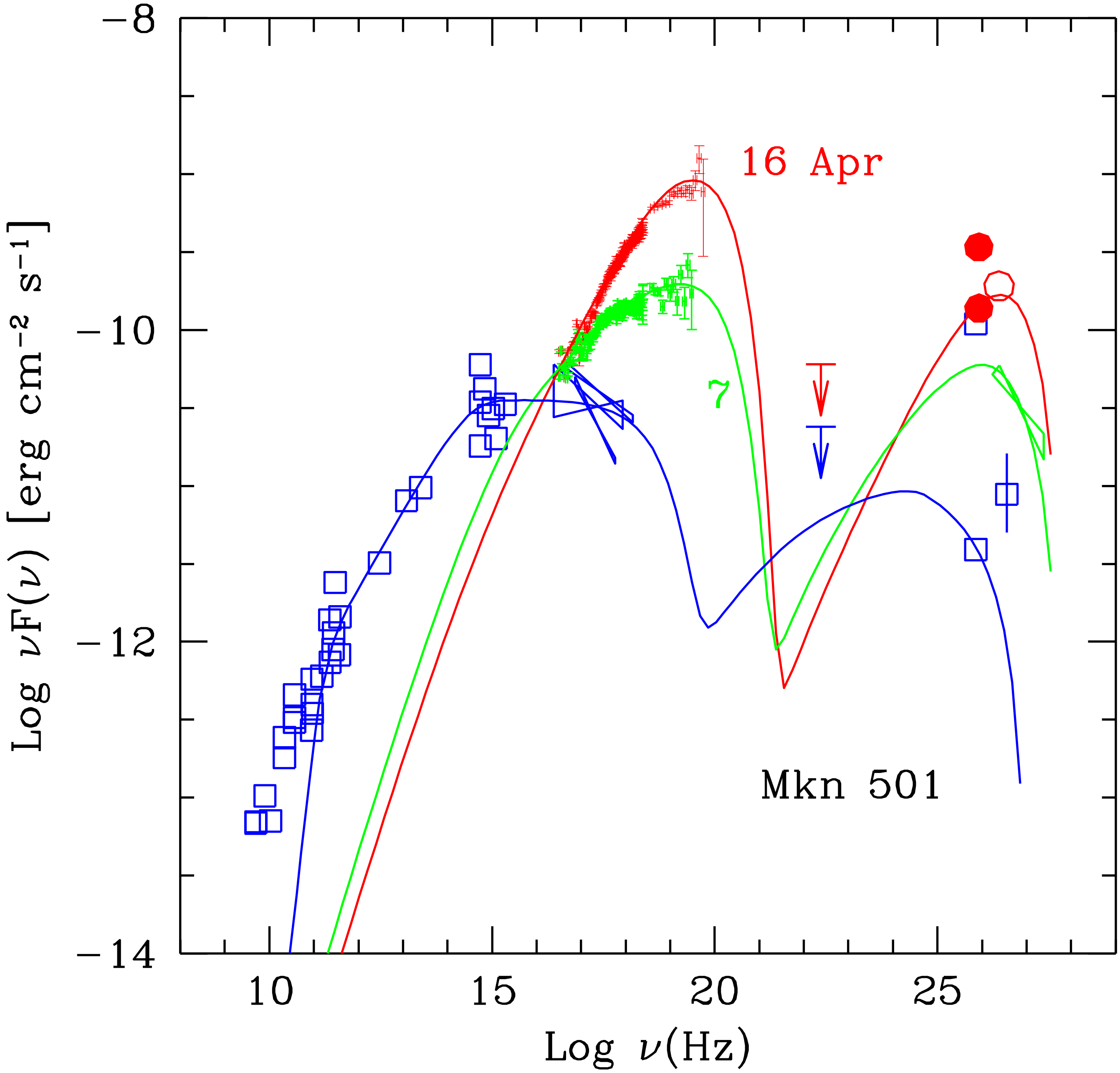

16 Apr
7
Mkn 501
Log νF(ν) [erg cm⁻² s⁻¹]
Log ν(Hz)
−8
−10
−12
−14
10
15
20
25